THE EFFECT OF BASELINE ESTIMATION ON ACCURACY OF INTERFEROMETRICALLY DERIVED DIGITAL ELEVATION MODELS

Premalatha BALAN
University of Nottingham,
Nottingham, England
balan@geography.nottingham.ac.uk

KEY WORDS: Interferometric Processing, SIR-C - IfSAR, Digital Elevation Model.

ABSTRACT

Interferometric SAR (InSAR) is being studied extensively to evaluate its potential to generate high resolution and high accuracy Digital Elevation Models (DEM). The accuracy of derived height information depends on many factors, including processing parameters, which need critical evaluation. Among the many processing parameters, baseline estimation requires a detailed evaluation of the methods used, as any inaccuracy in baseline estimation introduces a residual slope in the final DEM. Methods using orbital information to estimate the baseline are appropriate if the orbital information is precisely known. In the absence of such knowledge, other methods of estimating the baselines are required, and these are discussed in the present study. Fringe rate method depend on the location and size of the estimation window, as this method assumes that the fringes within the estimation window are due entirely to the phase trend on a flat earth. Baseline estimate using the fringe rate method or image offset parameters also fail to provide an accurate estimation of the baseline when the perpendicular and parallel components are estimated using the same method. However, fringe rate methods provide the best estimate for the perpendicular baseline component when compared to other methods studied. It is found that the use of the fringe rate method to estimate the perpendicular component of the baseline and the use of image offset parameters to estimate the parallel component of the baseline provides better results. Other methods gave "tilted" DEMs due to the presence of residual slope.

1 INTRODUCTION

Interferometric Synthetic Aperture Radar (InSAR) is, in theory, a source for accurate Digital Elevation Model (DEM) generation. In practical applications, the achievable accuracy varies depending on many factors. It is necessary to evaluate the factors governing the accuracy of the InSAR derived DEM to bring the technology to operational use.

The backscattered radar signal carries information about the target in the form of amplitude and phase, where amplitude is the strength of the signal and phase is the angular distance travelled by the signal from the antenna to the target and from the target back to the antenna. Information about the elevation of the target is contained in the phase content of the signal. To retrieve this information, two images of the same area collected from different observation points are processed by a series of steps. The DEM derived from InSAR processing and the expected (theoretical) InSAR DEM do not always match. The differences are due to the effects of different factors during processing. Estimation of baseline (the distance between the two observation points) is one of those factors which seriously affects the accuracy of the InSAR-derived DEM. Zebker et al. (1993) point out that inaccurate baseline estimation as one of the two main error sources in interferometrically-derived DEMs. The other major error source is phase noise. Though many researchers have mentioned the importance of accurate baseline estimation, the problem has not been addressed in detail. The reason could be that most of the evaluation experiments that have been conducted were dealing either with less sloping areas or relatively flat terrain where some inaccuracy in baseline estimation could have gone unnoticed. As InSAR is a potential source for high accuracy and high resolution DEMs, it is essential to address the effect of every processing parameter that affects the quality of the derived DEM. Significance of baseline estimation on the accuracy of InSAR derived DEM is addressed in this study.

Graham (1974) introduced the use of interferometry for topographic mapping in 1974. Later, Zebker et al. (1986) demonstrated the potential of the technique with practical results. They achieved a vertical accuracy of 10m using airborne data. The main source of error in their study was aircraft attitude. Since then many publications have reported different figures of height accuracy under different conditions. It is necessary to understand the causes of error and the conditions under which the accuracy was achieved (wavelength used, baseline separation, terrain nature etc.), otherwise the single figure reported as the accuracy of the InSAR-derived DEM is misleading. Other than system parameters and terrain characteristics that affect the achievable accuracy of the DEM, InSAR processing also affects the quality of the final derived DEM significantly.

1.1 Phase trend due to flat earth

The fringe pattern of a hypothetically perfect flat terrain should be uniform with a fringe rate depending only on the baseline separation between the satellite positions at which the master and slave images were acquired. A shorter baseline produces a low fringe rate, i.e. widely spaced fringes, whereas a longer baseline produces an interferogram with a high fringe rate, i.e. closely spaced fringes. This uniform fringe pattern gives an impression of uniform slope for this hypothetically flat terrain. This phase variation is called *phase trend due to flat earth.* To arrive at phase variation due to terrain height variations only, we need to remove the phase trend due to flat earth very accurately, as any inaccuracy in this process would lead to the introduction of a residual slope in the final DEM. To remove the flat earth phase trend, an accurate baseline estimate is required.

The baseline can be estimated from orbital information for the master and slave images. The co-ordinates of the orbital position are given in the leader file in the form of state vectors. Baseline estimation using state vectors would be the appropriate method if these vectors truly represented the satellite positions. The European Space Agency (ESA) provides four types of state vectors with different accuracy levels, details of which and of the accuracy associated with them can be found at ESA's website (http://earthent.esrin.esa.it). A brief description is provided here.

The types of state vectors provided by ESA are predicted orbits, restituted (or operational) orbits, preliminary orbits and precise orbits. *Predicted orbit* is calculated using fast delivery altimeter data from the last three days to predict the orbit for the next nine days. These estimates are updated daily to improve accuracy. The error of prediction is about 400m for a 6-day prediction, around 125 m for 3-day prediction and 25 m for 1-day prediction. The *restituted orbit* information is calculated using the predicted orbits and the orbital information of the central day of a three-day moving window. As a result, this information is available with a one-day delay after the satellite pass. The accuracy estimated is 2 – 4 m along track, and 1 – 2 m across track. *Preliminary orbits* are calculated on the basis of fast delivery tracking data for every 120 seconds with a spatial resolution of 900 km. *Precise orbit* results from a computation all available satellite tracking data and is corrected using dynamic models. The radial accuracy is in the order of 8-10 cm. This is the most accurate state vector available from ESA. Closa (1998) has studied the error introduced by inaccurate baseline estimations using different state vectors mentioned above, and suggests that very precise orbital information is needed to remove the residual phase due to flat earth. He also noted that additional altimeter data would improve the precision of the position of the orbit, even when precise state vectors are provided.

1.2 Methods of estimating baseline

When a user obtains data from a data provider, information about the type of state vectors provided in the leader file may not be available. If the state vectors are not of "precision" type, then an alternative method is needed to estimate the baseline. The Gamma software used in this study provides the user an opportunity to estimate baseline length using one of the following methods:

(a) Orbital information
(b) Image offset polynomial developed during co-registration of the SLC images
(c) Fringe rate method, and
(d) Combinations of the above methods.

It is reported in the Gamma documentation that baselines estimated using orbital information could be used as an initial estimate to input to other methods of baseline estimation, if the orbital information provided in the form of state vectors is not accurate. The methods using image-offset parameters use the image offset polynomial developed for the co-registration of the slave image to the master image, to estimate baseline separation. This method estimates the parallel baseline component more accurately than other methods. The fringe rate method uses the fringe rate in the interferogram over a flat terrain to estimate the baseline. The assumption in the second method is that the terrain covered by the estimation window is completely flat and that any fringe rate within this window is considered as the phase trend due to flat earth. This method estimates the perpendicular baseline component more accurately if the estimation window is positioned over a flat terrain of negligible slope (or negligible height variation) and if the window size is carefully specified in such a way that it is small enough to cover the area of flat terrain and large enough to allow the calculation of a stable estimate. Iterative estimations over different flat terrain windows positions and different flat terrain window sizes and combining all the estimates to produce a final baseline estimate would improve the results. However, this method estimates the parallel component very poorly. Combining different baseline estimation techniques is suggested as a method to improve the final baseline estimate. Using offset information to estimate the parallel component and using the fringe rate method to estimate the perpendicular component is believed to be the best combination for accurate baseline estimation.

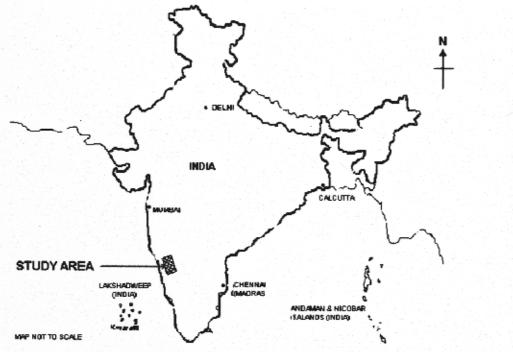

Figure 1 Location map of the study area

2 STUDY AREA AND DATA USED

The study area is part of Western Ghats of India and is shown in Figure 1. The area is covered between 75° 20′ E to 75° 25′ E longitude and 13° 11′ N to 13° 15′ N latitude. The area is covered by dense rain forest and the topography shows slopes of more than 40%, together with some cliffs. Coffee is the common crop cultivated in plantations along the hill slopes.

Data acquired by the SIR-C instrument flown on the Shuttle mission during 1994 were acquired for interferometric analysis. Optical data acquired by the PAN sensor mounted on the Indian Remote Sensing satellite IRS-1D was also used for this study. A 1:50,000 scale topographic map of the area was used to generate the reference DEM from 20m interval contours. The data sets used are listed in Table 1.

Platform	Sensor	Wavelength	Date of acquisition
SIR-C	SAR	23.5 cm (L band)	08 October 1994
SIR-C	SAR	23.5 cm (L band)	09 October 1994
IRS-1D	PAN	0.4 μm – 0.7 μm	17 December 1997

Table 1 Dataset used

3 METHODOLOGY

3.1 Baseline estimation using state vectors

Interferometric processing consists of a series of steps to generate a DEM from a pair of Single Look Complex (SLC) data. As a first step, the SLC images were co-registered to sub-pixel accuracy using one image as the reference (master) image and the second as the slave image. A complex interferogram is generated from the co-registered SLC images by multiplying the complex value of the master image with the complex conjugate of the slave image on a pixel by pixel basis. The phase value of this complex interferogram (Figure 2) is proportional to the height of the terrain. The wrapped phase of the interferogram contains the phase due to flat earth in addition to phase component determined by the height of the terrain. To remove the phase component due to flat earth, the baseline was estimated using orbital information provided in the leader file of the data set in the form of state vectors. The resultant interferogram (the “flattened interferogram”) is shown in figure 3(a). The flattened interferogram was then unwrapped and converted to terrain heights by inputting a number of ground control points. This elevation image, which was in slant range geometry, was then orthonormalised to ground geometry. The orthonormalised height image is the InSAR derived DEM.

3.1.1 DEM comparison

To evaluate the effect of any processing parameter, it is necessary to have a reference DEM, ideally the theoretical InSAR DEM. In the absence of the theoretical InSAR DEM, another DEM derived from established methods could be used as the reference DEM. In this case the differences are not only due to the processing parameter but due to other factors as well. The other factors that affect the quality of the DEM are system parameters and the terrain parameters. The system parameters include wavelength, actual (not estimated) baseline separation, pixel resolution and temporal baseline (time delay between the interferometric pair acquisition). Terrain parameters include vegetation density and type, meteorological conditions, and slope. If the processing parameter introduces systematic error then height differences due to system parameters and the terrain parameters can be ignored. In this study, a DEM generated from 20m contours in a 1:50,000-scale map was used as the reference DEM. These contours were digitised using the Arc/Info software package. Spot heights were also digitised. The DEM was generated by triangulation method using the ERDAS Imagine software package.

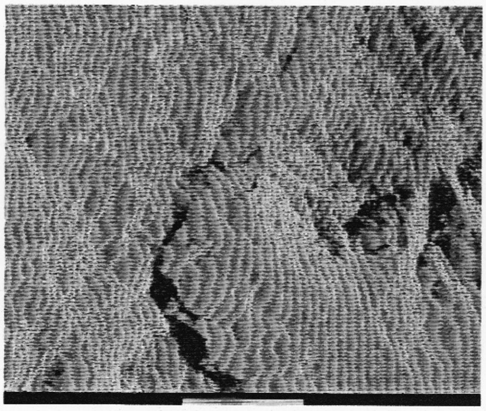

Figure 2 Interferogram with phase trend due to flat earth

To compare the InSAR DEM and the reference DEM it is necessary for the InSAR DEM to be geo-referenced. Registering DEMs is a difficult task as there are no well-defined ground control points in the smoothly undulating height values of the DEMs. In order to register the InSAR-derived to the reference DEMs, the amplitude image (which is in the same geometry as the InSAR DEM) was registered to the map to produce a registration polynomial between SAR geometry and map geometry. This registration polynomial is then used to transform the InSAR derived DEM to map geometry. As the amplitude image for the study area did not have many well-identifiable ground control points, the PAN image from the IRS-1D satellite was first registered to the map, since the PAN image had many well identifiable cultural features which are also shown in the map. The amplitude image was then registered to the PAN image. The PAN image and the SAR amplitude image had some well identifiable feature in common. In order to achieve the best possible interpretability, the coherence and amplitude images for both the SLC images were added to generate a colour composite image. This composite is registered to the PAN image that is in the map geometry. The registration polynomial developed to register the InSAR colour composite image to the PAN image is used to transform the InSAR DEM to map geometry.

A common area between the registered DEMs was cut from larger images in order to compare height differences between the DEMs. The registered InSAR DEM is subtracted from the reference DEM to generate a difference image. This difference image showed systematic height differences, i.e., there was an increase in height difference from West to East of the image. This indicated a tilt in the InSAR DEM due to an inaccuracy in a processing parameter.

3.2 Baseline estimation using other methods

The systematic height difference could be removed by two ways. One is by estimating the tilt from the difference image and removing it by adding a tilt component to every pixel in the DEM. Alternatively, the reason for the tilt could be analysed. Determining the source of the tilt is more important than just removing it by estimating from the tilted DEM. Careful analysis of each step of the InSAR processing chain revealed that the tilt was due to inaccurate baseline estimation.

The state vectors provided in the leader file do not appear to represent the orbital positions of the Shuttle very precisely, hence it is necessary to estimate the baseline from the image and/or interferogram parameters. Other methods of baseline estimation attempted are listed below.

1. Orbital information was used to estimate both perpendicular and parallel components.
2. Image offset parameters were used to estimate both perpendicular and parallel components.
3. The fringe method was used to estimate both perpendicular and parallel components with default estimation window location (centre of the image) and default window size (512 in range and 1024 in azimuth).
4. The fringe rate method was used to estimate both perpendicular and parallel components by choosing a window location over a relatively flat area with a window size that covers just the flat area chosen.
5. The fringe rate method was used to estimate the perpendicular baseline component with estimation window used in method 4, and orbital information was used to estimate the parallel baseline component.
6. The fringe rate method was used to estimate the perpendicular baseline component with estimation window used in method 4, and image offset parameters were used to estimate the parallel baseline component.

Method	**Perpendicular component (m)**	**Parallel component (m)**
1. Orbital information is used for both the components	139.2467	-31.2750
2. Offset information is used for both the components	143.7984	-40.7094
3. Fringe rate method is used to estimate both the components when the estimation window is at the centre with the default window size (512 in range and 1024 in azimuth)	123.7560	-0.0060
4. Fringe rate method is used to estimate both the components by placing the window over a flat area with a user defined window size. The area and the window size were selected by analysing the contour pattern in the map.	150.2302	0.0500
5. Orbital information is used to estimate the parallel component and fringe rate method is used to estimate the perpendicular component. The fringe estimation window was the same as the one used in method 4.	149.9380	-31.3780
6. Offset information is used for parallel component and fringe rate method is used to estimate the perpendicular component. The fringe estimation window was the same as the one used in method 4.	149.9669	-40.7688

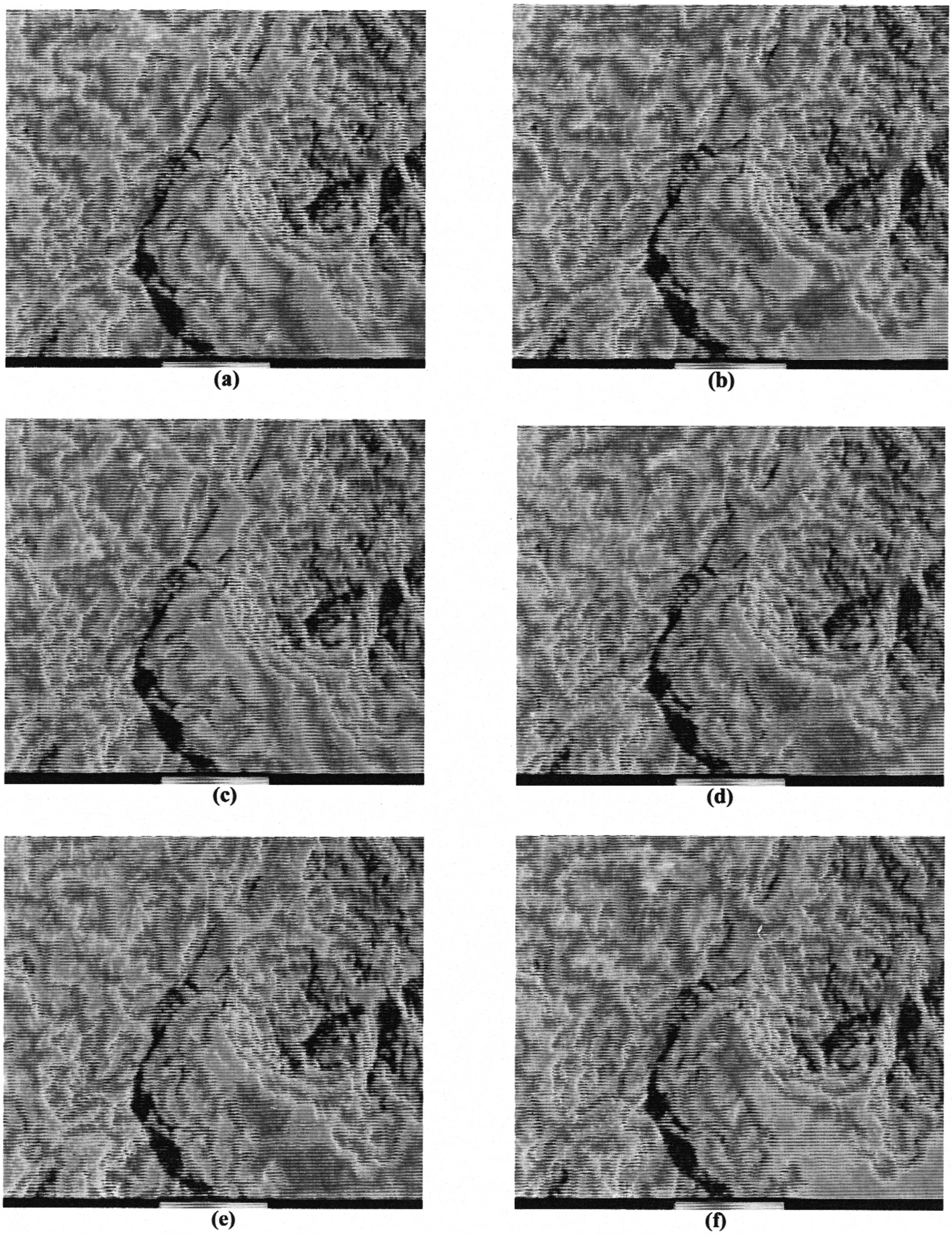
(a) (b) (c) (d) (e) (f)

Figure 3 Flattened interferograms using **(a)** baseline estimate based on orbital information, **(b)** using baseline estimate based on image offset information, **(c)** baseline estimate using fringe rate method with default estimation window size and default window location, **(d)** baseline estimate using fringe rate method by placing the estimation window over a flat location, **(e)** baseline estimate using fringe rate method to estimate perpendicular baseline component and orbital information for parallel component and **(f)** baseline estimate using fringe rate method to estimate the perpendicular baseline component and image offset parameters to estimate the parallel component

Baseline estimates for all these methods are listed in Table 2, and flattened interferograms for these baseline estimates are shown in Figure 3. The flattened interferograms were unwrapped to derive InSAR DEMs for all baseline estimates. There were six DEMs, including the one derived for baseline estimate using orbital information as a first trial. Since the DEM generated for baseline estimate using orbital information was already map-registered and differenced from the reference DEM, the other five DEMs were registered to the reference DEM as explained above, and differenced from the reference DEM. The results are discussed in the following section.

4 RESULTS AND DISCUSSION

Accurate baseline determination is one of the most important factors in determining the quality of InSAR derived DEM or any InSAR product. The method used to estimate the baseline is very important as further processing based on the estimated baseline significantly affects the quality of the final product. In this study, baselines were estimated using orbital information, image offset parameters, fringe rate method and combinations of these methods, producing six flattened interferograms using six different baseline estimates as mentioned above. All the six flattened interferograms using these baseline estimates follow to some extent the actual terrain topography as depicted on the map, though they differ from each other (Figure 3). Close examination and inter-comparison of the interferograms shows a number of discrepancies in the height values from the interferogram (by counting the fringes) for a few selected locations and actual height values shown in the map for the same locations. When DEMs were generated from these interferograms, the differences became very obvious. DEMs generated using the baseline value from the fringe rate method to estimate both perpendicular and parallel components of the baseline (method 3 and method 4), contained discontinuities (holes) located near the centre of the image, irrespective of the fringe estimation window location. This may be due to an inaccurate parallel component estimated by fringe rate method, which is a known disadvantage of this method (reported in Gamma software documentation). These two DEMs were ignored for further comparison. The other four DEMs registered to the reference DEM and a common area was cut from all these DEMs. Four InSAR DEMS were subtracted from the reference DEM to generate respective difference images. The difference images showed tilt in different directions. The degree of tilt can be arrived at by taking profiles along the locations of lowest value and highest values in the difference images. The profiles and the profile locations for each image are shown in figures 4 to 7. Since the profiles for tilt were taken along different directions and for different locations, cross sections of all four DEMs and for the reference DEM, for same location in all images (along East-West direction of the image) were taken and are shown in Figure 8.

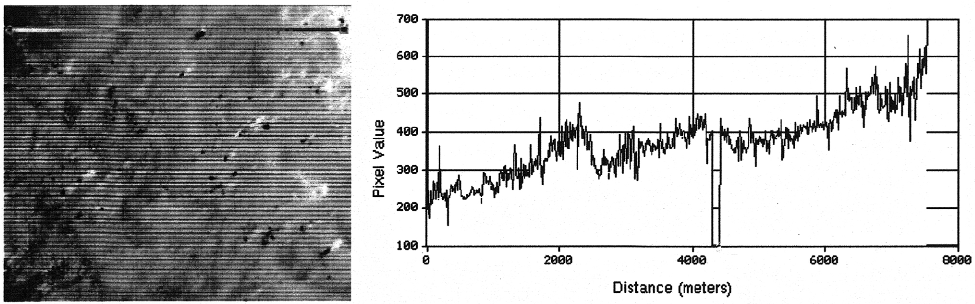

(a) (b)

Figure 4 Profile along the tilt of the DEM generated using baseline estimate based on orbital information. **(a)** profile location and **(b)** the profile in the tilt direction

Figure 4(a) shows that the tilt in the DEM generated using orbital information was in an east-west direction, with lower value in the west and higher value in the east. The difference values for this DEM were above zero as seen from Figure 4(b), meaning that the datum of the InSAR DEM was below the datum of the reference DEM (mean sea level), with a tilt in east-west direction. This is evident from the cross section of the InSAR DEM in comparison with the reference DEM shown in Figures 8(a) and 8(e) respectively. For the cross section shown in the Figure 8(a), the height values in the InSAR DEM for the baseline estimate based on orbital information were 300m below the reference DEM value in the west-most location and 500m below the reference DEM in the east-most location. Note that the shape of the InSAR DEM agrees with the shape of the reference DEM if the noise and the hole in the InSAR DEM are overlooked.

The InSAR DEM generated using a baseline estimate derived from image offset parameters showed a northwest-southeast tilt with the lowest value in the southeast location and the highest value in the approximately northwest location, as shown in Figure 5(a). The degree of tilt is almost same (Figure 5(b)) as that of DEM generated using baseline estimate based on orbital information (Figure 4(b)) but the direction of tilt is different. When we compare the cross section of the DEM, then the DEM with image offset parameters used for baseline estimation shows a lower level datum. The height value of the InSAR DEM in the west-most location is 400m below the height value of the reference DEM and height value in the east-most location is 300m below the reference DEM (Figure 8(b) and 8(e)). In this case also, the shape of the DEM agrees with shape of the reference DEM, while there are noise and holes as in the previous case.

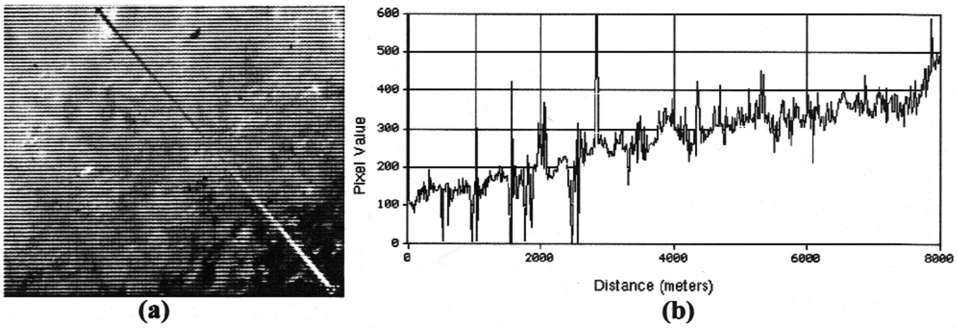

(a) (b)

Figure 6 Profile along the tilt of the DEM generated using baseline estimate based on image offset parameters. **(a)** Profile location and **(b)** the profile along the tilt

The DEM generated using the fringe rate method to estimate the perpendicular baseline component and orbital information used to estimate the parallel component showed less tilt compared to the previous two cases. Also the datum of the InSAR DEM is above the level of the datum of the reference DEM which is evident from Figure 6(b) where the profile of the difference image starts with a negative value. If we look at the DEM cross section shown in Figure 8(c) the height value of the InSAR DEM in the west-most location is just 100m below the height value of the reference DEM whereas the east-most location has a height value almost equal to the height value of the reference DEM. The difference image still shows a considerable tilt (Figure 6(b)), and the profile exhibits an increasing trend from top to bottom of the image (Figure 5(a)) which is shown as left to right in the profile in Figure 6(b). In this case also the shape of the DEM profile agrees well with the shape of the profile of the reference DEM, when the presence of noise and holes are ignored.

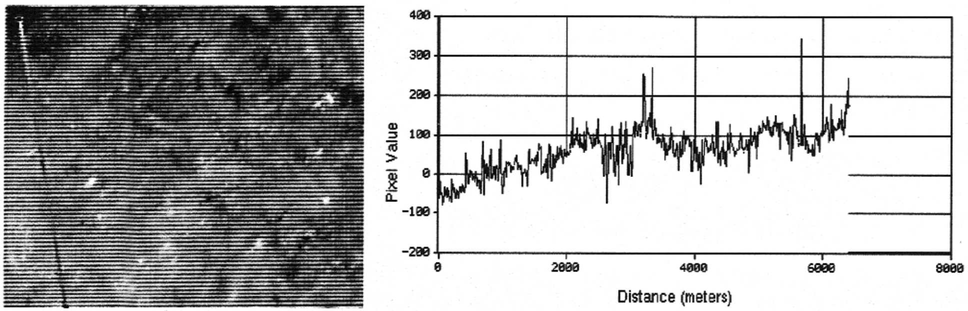

(a) (b)

Figure 5 Profile along the tilt of the DEM generated using baseline estimate based on fringe rate method to estimate the perpendicular component and orbital information to estimate the parallel component of the baseline. **(a)** Profile location and **(b)** the profile along the tilt

The DEM generated using the fringe rate method to estimate the perpendicular component and image offset parameters to estimate the parallel component of the baseline showed less tilt when compared to all other DEMs, though there is still some tilt in the difference image (Figure 7(b)). The cross section of the InSAR DEM shows a good agreement with the cross section of the reference DEM. The west-most height value in Figure 8(d) is just in the level of the reference DEM height value in Figure 8(e), whereas the east-most height value little higher than the reference DEM height value (Figure 8(d) and Figure 8(e) respectively). The shape of the InSAR DEM shows as very good agreement with the shape of the reference DEM even for the smaller undulations in the DEM cross section. The tilt still present in this DEM can be removed by many ways. One of them can be the iterative methods of locating the flat window for the fringe rate method. If the fringe estimation window is not perfectly flat, which is the case of the most of the "real world" situations, the estimated baseline would produce either an under-estimated or an over-estimated value, depending upon the direction of the slope within the fringe rate estimation window, with respect to the look direction of the SAR systems. Another method can

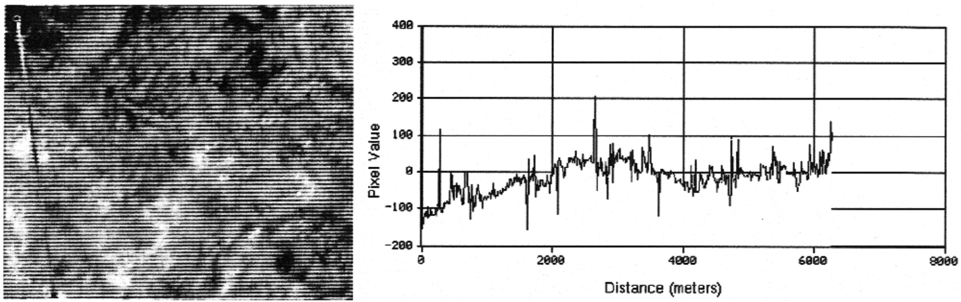

(a) (b)

Figure 7 Profile along the tilt of the DEM generated using baseline estimate based on fringe rate method to estimate the perpendicular component and image offset parameters to estimate the parallel component of the baseline. **(a)** Profile location and **(b)** the profile along the tilt be to use the precision estimate based on the input ground control points as the initial estimate and repeating the whole process starting from flattening the interferogram. This method may improve the results. Another method is to use a different set of ground control points for precision baseline estimation. A combination of any of the above mentioned methods may also improve the quality of the final DEM.

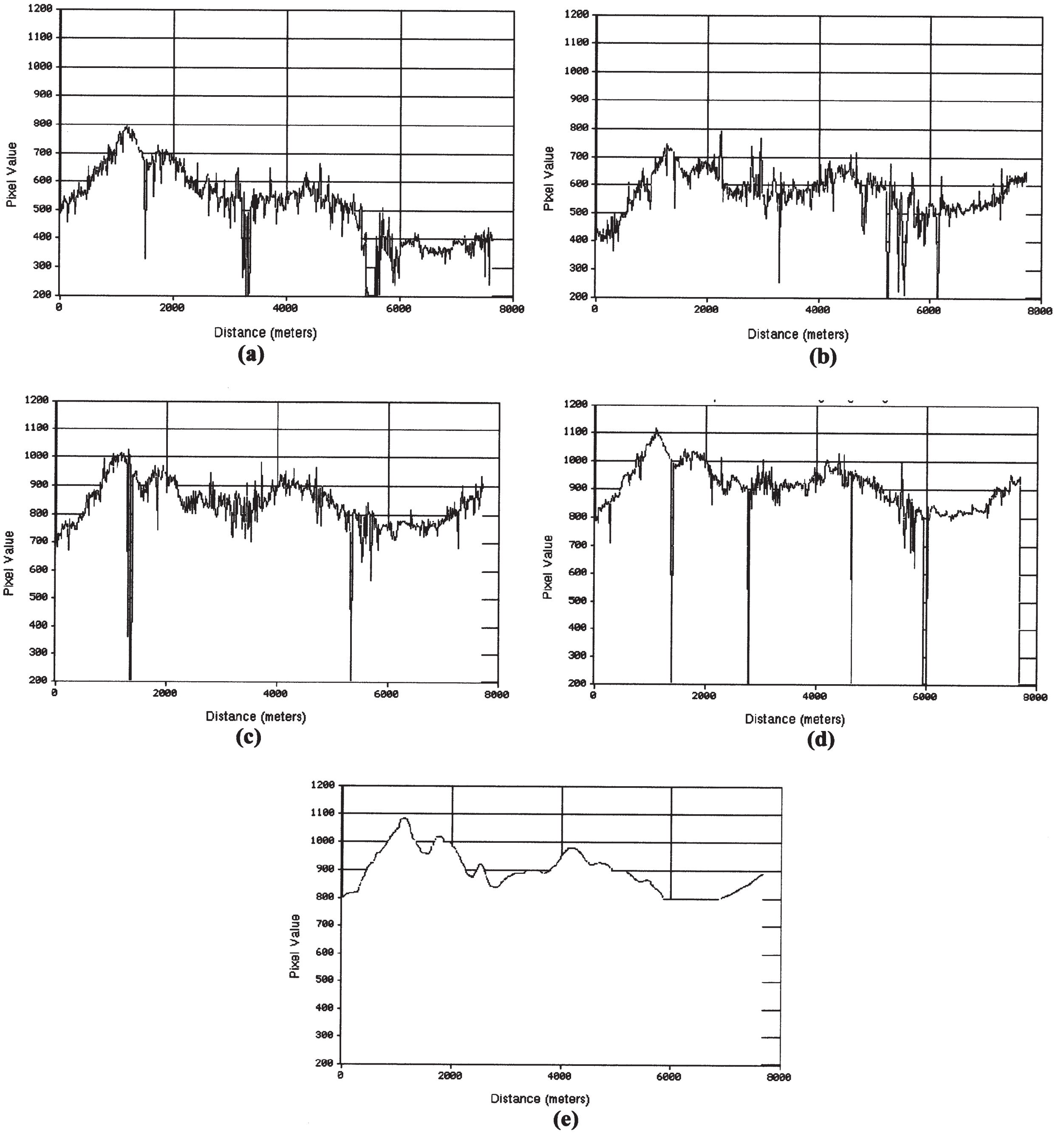

(a)

(b)

(c)

(d)

(e)

Figure 8 Profiles for the cross section along East –West direction of the DEMs. **(a)** Profile for the DEM generated using baseline estimate based on orbital information. **(b)** Profile for the DEM generated using baseline estimate based on image offset parameters. **(c)** Profile for the DEM generated using baseline estimate based on fringe rate method to estiamte th eperpendicular component and orbital information to estimate the parallel component. **(d)** Profile for the DEM generated using baseline based on fringe rate method to estiamte the perpendicular component and image offset parameters to estiamte parallel component. **(e)** The profile for the reference DEM

5 SUMMARY AND CONCLUSION

The effects on DEM quality of estimating baseline using different methods are discussed. Baseline estimates using orbital information, provided in the leader file of the data, give a DEM with a residual slope. Also, the datum of the resulting DEM, in this case study, is well below the datum (mean sea level) of the reference DEM. Baseline estimate using image offset parameters also shows a similar trend but with a tilt in a different direction. If the fringe rate method is used alone produces discontinuities in the DEM because of poor estimation of the parallel component of the baseline. When combined with orbital parameters or image offset parameters to estimate the parallel baseline component, the fringe rate method provided comparatively better results, provided the fringe rate estimation window is placed over flat terrain only. Iterative methods of locating the best window location and best window size would reduce the tilt in the final InSAR DEM.

ACKNOWLEDGEMENTS

The author is grateful to her supervisor Prof. Paul M. Mather, University of Nottingham, for his guidance. The author also expresses her gratitude to NASA JPL for providing the SIR-C data, and to Prof. P.S. Roy and Mr. P.L.N. Raju, IIRS, Dehradun, India, for providing the Survey of India topographic map and IRS-1D PAN data for this study. The study is supported by a Commonwealth Scholarship. Computing facilities were made available by the School of Geography, University of Nottingham.

REFERENCES

Closa, J., 1998. The Influence of orbit precision on the quality of ERS SAR interferometric data. http://earth1.esrin.esa.it/ORB_QL (1 June 1998).

Graham, L.C., 1974. Synthetic Interferometer Radar for topographic mapping, Proceedings of the I.E.E.E., 62, pp.763-768.

Zebker, H.A., and Goldstein, R.M., 1986. Topographic mapping from interferometric Synthetic Aperture Radar observations. Journal of Geophysical Research, 91, pp.4993-4999.

Zebker, H.A., Werner, C.L., Rosen, P.A., and Hensely, S., 1994. Accuracy of topographic maps derived from ERS-1 Interferometric Radar. I.E.E.E. Transactions on Geoscience and Remote Sensing, 32(4), 823-836.